Original Research Article

Bioadhesive floating microsponges of cinnarizine as novel gastroretentive delivery: Capmul GMO bioadhesive coating versus acconon MC 8-2 EP/NF with intrinsic bioadhesive property

Smita Raghuvanshi, Kamla Pathak

Department of Pharmaceutics, Rajiv Academy for Pharmacy, Chhatikara, Mathura, Uttar Pradesh, India

Abstract

Introduction: The study was aimed at the development of low-density gastroretentive bioadhesive microsponges of cinnarizine by two-pronged approach (i) coating with bioadhesive material and (ii) exploration of acconon MC 8-2 EP/NF as bioadhesive raw material for fabrication. **Materials and Methods:** Microsponges were prepared by quasi-emulsion solvent diffusion method using 3^2 factorial design. Capmul GMO was employed for bioadhesive coating. In parallel, potential of acconon for the fabrication of bioadhesive floating microsponges (A8) was assessed. **Results:** Formulation with entrapment efficiency = 82.4 ± 3.4%, buoyancy = 82.3 ± 2.5%, and correlation of drug release (CDR_{8h}) = 88.7% ± 2.9% was selected as optimized formulation (F8) and subjected to bioadhesive coating (BF8). The $\%CDR_{8h}$ for A8 was similar to BF8 (87.2% ± 3.5%). Dynamic *in vitro* bioadhesion test revealed comparable bioadhesivity with BF8. The *ex vivo* permeation across gastric mucin displayed 63.16% for BF8 against 56.74% from A8; affirmed the bioadhesivity of both approaches. **Conclusion:** The study concluded with the development of novel bioadhesive floating microsponges of cinnarizine employing capmul GMO as bioadhesive coating material and confirmed the viability of acconon MC 8-2EP/NF as bioadhesive raw material for sustained targeted delivery of drug.

Key words: Acconon MC8-2 EP/NF, capmul GMO, cinnarizine, dynamic *in vitro* bioadhesion test, *ex vivo* permeation, microsponges

INTRODUCTION

Cinnarizine, a piperazine derivative, is a calcium channel blocker used in the treatment of vertigo, motion sickness, and vomiting. It is a weak base with poor aqueous solubility (<1 μg/ml),[1] extensively absorbed from the upper part of the gastrointestinal tract. A major limitation associated with cinnarizine is gastric acid-dependent solubility, which accounts for low and erratic bioavailability.[2-4] Various gastroretentive systems of cinnarizine have been cited in literature that describes both single and multiple unit dosage forms. Although single unit systems provide effective gastroretention, multiparticulate systems are preferred due to high degree of dispersion in digestive tract, lesser risk of dose dumping,[5] and capable of passing through gastrointestinal tract readily, leading to less inter- and intra-subject variability.[6]

The research reports on gastroretentive multiparticulate systems of cinnarizine include floating microballoons,[7] floating microspheres,[8] and mucoadhesive microparticles.[9] Despite promising gastroretention, the results were compromised by low drug loading capacity (20–40%). This guided the selection of microsponges as a superior delivery system. Microsponges

Address for correspondence:
Dr. Kamla Pathak,
Department of Pharmaceutics, Rajiv Academy for Pharmacy,
P. O. Chhatikara, Mathura - 281 001, Uttar Pradesh, India.
E-mail: kamlapathak5@gmail.com

Access this article online

Quick Response Code:

Website: www.jpionline.org

DOI: 10.4103/2230-973X.195923

How to cite this article: Raghuvanshi S, Pathak K. Bioadhesive floating microsponges of cinnarizine as novel gastroretentive delivery: Capmul GMO bioadhesive coating versus acconon MC 8-2 EP/NF with intrinsic bioadhesive property. Int J Pharma Investig 2016;6:181-93.

appear to be advantageous, with high drug loading capacity of about 50–60%[10] due to numerous interconnected pores that can adsorb high quantity of active on the surface and/or load to the bulk of particle. This system provides maximum efficacy, extended product stability, reduced side effects, and favorably modifies drug release.[11] Microsponges also have the ability of entrapping drugs in the pores, thus improving the rate of solubilization of poorly water-soluble drugs.[12] This in addition provides the advantage of reduced dose administration. To the depth of our knowledge, the literature lacks well-described reports on the microsponges of cinnarizine, which suggested for the development of floating ethyl cellulose (EC) microsponges of cinnarizine as a novel addition to the previous studies on floating system of cinnarizine.

The floating ability of microsponges has already been proven in a research outcome from our laboratory, wherein floating curcumin-loaded microsponges were formulated and assessed.[13] The research reported high drug loading capacity (66.94%) of microsponges prepared by modified quassi emulsion solvent diffusion method. Although microsponges emerged as novel floating system, like other multiparticulate systems, they also suffer from the risk of being expelled out from the stomach due to migrating myoelectric complex motility wave. This may be overcome by bioadhesive floating microsponges that can extend the gastroretention either partially/wholly.[14] This led to focus on the extension of floating EC microsponges of cinnarizine as a new bioadhesive floating system.

Based on these considerations, the objective of the present study was (a) to optimize drug loading capacity floating EC microsponges of cinnarizine by 3^2 factorial design using critical micelle concentration (CMC) as a key for the selection of polymeric surfactant and (b) to develop bioadhesive system of the optimized formulation to enhance gastroretention that may improve patient compliance by minimizing fluid intake. For the latter, two-pronged approach has been implicated: (i) conventional coating with bioadhesive material and (ii) novel exploration of acconon MC 8-2 EP/NF (PEG-8 caprylic/capric glyceride) as bioadhesive raw material for the fabrication of bioadhesive floating microsponges.

MATERIALS AND METHODS

Materials

Cinnarizine (I.P.) was received from Ray Chemicals (p) Ltd., Bangalore, India. EC (lot no: 02129) was purchased from the Central Drug House (P) Ltd., New Delhi, India, and polyvinyl alcohol (PVA) (lot no: RM 6170) was purchased from Himedia, New Delhi, India. PEG-8 caprylic/capric glycerides (brand name: acconon MC 8-2 EP/NF, Lot no. 090612-8) and glycerol monooleate (brand name: Capmul GMO, Lot no. 100616-8) were obtained from ABITEC Corporation, Janesville, WI, USA. Ethanol (lot no: XK-13-201-00185) and dichloromethane (lot no: R271J06) were obtained from S D Fine-Chem Limited, Mumbai, and Rankem, India, respectively. All other chemicals were procured from local sources and are of high purity.

Methods

Critical micelle concentration

CMC of polymeric surfactant; PVA was determined by measuring surface tension by drop count method using Traube's stalagmometer.[15] Aqueous solutions of PVA of varying concentrations (0.05%, 0.1%, 0.2%, 0.4%, 0.5%, 1%, and 2% w/v) were prepared. Fixed amount of sample solution was delivered as freely falling drops from the capillary end of stalagmometer, and the number of drops was counted. The surface tension was measured against water as reference. CMC was determined graphically by plotting between surface tension versus concentration.

In vitro drug adsorption

The test was conducted on polymeric carrier, EC. An excess quantity of cinnarizine (10 mg) was added to 100 ml of phosphate buffer, pH 4.5. A 10-fold weight of EC granules was added to form homogenous dispersion and it was magnetically stirred at 100 rpm at a temperature of 30 ± 2°C for 12 h. Samples were withdrawn at 0, 1, 2, 4, 6, 8, and 12 h, filtered and analyzed spectrophotometrically (Shimazdu, Pharmaspec 1700, Tokyo, Japan) at 251 nm. Results were interpreted graphically from the plot between percent drug adsorbed versus time. The experiment was repeated for different concentrations of EC (0.3%, 0.6%, and 0.9% w/v) at similar conditions. Paired Student's *t*-test ($P < 0.01$) was applied between each sampling time as well as the three concentrations of EC to determine the optimum stirring time and concentration(s) of EC required for the preparation of microsponges.

Preparation of drug-loaded microsponges

Microsponges were prepared by quasi emulsion solvent diffusion method,[16] consisting of inner and outer phases. Inner phase was prepared by dissolving cinnarizine and EC in 20 ml of dichloromethane and ethanol (95%) used in a ratio of 1:1. An outer phase containing aqueous solution of PVA (100 ml) was prepared separately and inner phase was added dropwise into it at 30 ± 2°C under continuous stirring (500 rpm). The o/w emulsion was stirred for 6 h on magnetic stirrer at the same stirring speed. The mixture was filtered to separate microsponges that were dried at 40°C in hot air oven and stored in desiccators till use. The microsponges were prepared using 3^2 factorial design, wherein the concentration of EC and PVA was designated as independent variables. A total of nine formulations were prepared, varying the amount of EC and PVA at three different levels (−1, 0, and + 1) whereas the amount of drug and organic solvents was kept constant [Table 1]. The dependent variables were percent entrapment efficiency, buoyancy, and percent cumulative drug release.

Evaluation of microsponges

Product yield and particle size

The product yield was calculated by dividing the weight of prepared microsponges to the total dry weight of drug and

Table 1: 3^2 factorial design for the formulation of cinnarizine-loaded microsponges

Formulation code	Cinnarizine (mg)	Ethyl cellulose (X1) (mg)	PVA (X2) (%w/v)	DCM ethanol (v/v)	Dependent variables
F1	100	−1 (300)	−1 (0.5)	1:1	Percentage of entrapment efficiency (Y1)
F2	100	−1 (300)	0 (1)	1:1	
F3	100	−1 (300)	+1 (1.5)	1:1	Buoyancy$_{8h}$ (%) (Y2)
F4	100	0 (600)	−1 (0.5)	1:1	Percentage of CDR$^{b}_{8h}$ (Y3)
F5	100	0 (600)	0 (1)	1:1	
F6	100	0 (600)	+1 (1.5)	1:1	
F7	100	+1 (900)	−1 (0.5)	1:1	
F8	100	+1 (900)	0 (1)	1:1	
F9	100	+1 (900)	+1 (1.5)	1:1	
F10[a]	100	0.5 (750)	0.5 (1.25)	1:1	

[a]Extra design checkpoint, [b]Cumulative drug release. PVA: Polyvinyl alcohol, DCM: Dichloromethane

excipients added to a particular formulation. The particle size was determined by dynamic laser scattering method using Beckman coulter LS 13 320 analyzer with optical model Fraunhofer. rf780z, USA. Water was used as dispersant. The suspension was added dropwise into the sample cell equipped inside the instrument. Addition of suspension of sample was continued up to obscuration rate of 3%. The graph was obtained between volume (%) versus particle diameter (μm), and calculation was done from 0.375 to 2000 μm. The data obtained were used to determine the size distribution.

Percent entrapment efficiency

Accurately weighed amount of microsponges were crushed and 10 mg of powder was dispersed in 5 ml of methanol followed by vortexing to extract the drug. This was centrifuged (R-4C, Remi centrifuge, Vasai, India) at 2000 rpm for 10 min and the filtrate was analyzed spectrophotomerically. Percent drug content and percent entrapment efficiency were calculated by the following equations:

$$\text{Percent entrapment efficiency} = \frac{\text{Practically entrapped drug}}{\text{Total amount of drug incorporated}} \times 100 \quad (1)$$

In vitro buoyancy

Hundred milligrams of accurately weighed microsponges was spread on 100 ml phosphate buffer, pH 4.5 containing 0.02% w/v tween 80. The floating systems remain buoyant under fed state condition, where pH varies in the range of 2.5–6.5 and pH 4.5 represented the intermediate fed state pH which was suitable to access the *in vitro* buoyancy test of microsponges. The use of tween 80 simulated the wetting effect imparted by naturally occurring surface active agent in gastrointestinal tract. The medium maintained at 37 ± 0.5°C was stirred magnetically (100 rpm). After 8 h, microsponges that remained floating over the surface of the medium were recovered, dried, and weighed. The percent buoyancy was calculated by the ratio of floating microsponges to the total microsponges added.

In vitro drug release

The release of drug from microsponges was determined by modified Rosette Rice apparatus.[17] An accurately weighed amount of microsponges equivalent to 10 mg of drug were placed in a modified beaker containing 70 ml of phosphate buffer, pH 4.5 with 0.02% w/v Tween 80. A pH of 4.5 represented the midpoint of fed state pH ranging from 2.5 to 6.5 was selected. The test was performed at 37 ± 0.05°C and 75 rpm. Samples of 2 ml were withdrawn at 0, 1, 2, 3, 4, 6, and 8 h and filtered. An equal volume of fresh media was added to maintain the sink condition. The samples were diluted appropriately and assayed spectrophotometrically at 251 nm to analyze the drug released in dissolution media. Graph was plotted between percent cumulative drug release and time. The release data generated were subjected to zero order, first order, and Higuchi's model (s) to understand the release kinetics of cinnarizine from microsponges. The model with highest correlation coefficient was considered to be the best fitted for release profile. The data were also fitted in Korsmeyer Peppas model, and the value of diffusion exponent (n) was calculated to analyze the mechanism of drug release. Drug release was also studied in phosphate buffer, pH of 2.5 and 6.5, to assess the effect of simulated fed state conditions on the release of cinnarizine from the optimized formulation.

Statistical analysis

The response data of the experimental design were analyzed using Design Expert Software version 9 (Stat Ease, Inc., Minneapolis, USA) to summarize the effect of independent variables on dependent variables. The polynomial equations for percent entrapment efficiency, percent buoyancy, and percent cumulative drug release were generated by applying one way ANOVA after omitting the insignificant coefficients at 95% confidence level. The generated polynomial equations were used to predict responses at different levels of independent variables.

Selection of optimized formulation and validation of experimental design

The maximum desirability approach was employed to identify optimized formulation with maximum combined responses. The experimental design was validated by preparing an extra design check point formulation (F10). The formulation was experimentally evaluated for percent entrapment efficiency, percent buoyancy, and percent cumulative drug release. The polynomial equations generated were used to calculate the predicted responses for the respective three responses. The experimental and predicted responses were compared using paired t-test at 95% confidence interval ($P < 0.05$).

Bioadhesive microsponges

Bioadhesivity can be conferred to microsponges by two approaches: (a) bioadhesive coating and (b) use of bioadhesive raw material.

Bioadhesive coating

The optimized formulation (F8) was subjected to bioadhesive coating by solvent evaporation method employing capmul GMO-50 as a coating material. The microsponges of optimized formulation were dispersed in 5 ml of petroleum ether (40°C) containing 0.4% w/v of capmul GMO. Evaporation of solvent at 40°C coated the microsponges, which were stored in desiccator till further evaluation. Coated microsponges (BF8) were evaluated for all response parameters.

Bioadhesive raw material

Owing to the intrinsic bioadhesive property, acconon MC 8-2 EP/NF was selected for preparing microsponges. CMC of acconon MC 8-2 EP/NF, determined by the same method as described above, was stipulated as the concentration for the preparation of microsponges. The optimized formulation (F8) was reformulated using acconon MC 8-2 as polymeric surfactant. The formulation requirements were similar to that of F8 except that the level of EC was changed to 600 mg and a temperature of 20°C was maintained to get A8. Bioadhesive microsponges prepared employing two different approaches were assessed experimentally.

Dynamic in vitro bioadhesion

The test was performed to evaluate the bioadhesive property of microsponges in reference to the uncoated microsponges. For this purpose, a lab-fabricated device as described by our research team[18] was used. Briefly, two stainless steel plates (9.5 cm × 6.0 cm) were hinged together: a manually movable plate (A) and a base plate supported on spring fixed on a wooden plank. At the hinged position of the plates, vibrating DC motor (D/V 5.9 RF 300C-114400) driven by battery (9 V), with a current of 2.54 mA, was placed. A rheostat was used in the circuit to provide a frequency of 3–5 cycles/min to simulate peristaltic movement in the stomach. The base plank was attached to another vertical wooden plank. On the vertical plank, bolts were drilled at 0, 30, 45, 60, 75, 90, 120, and 180°. The goat stomach mucosa (8.5 cm × 5.5 cm) was mounted on the movable plate A that was made to move through variable angles for the experiment. Forty microsponges of BF8 were hydrated in phosphate buffer, pH of 4.5 for 30 min, and placed over the mucosa, resting at 0°. Plate A was made to move at 30° and allowed to vibrate for 3 min. The movement of the microsponges was carefully observed and recorded. The plate was then moved to 45, 60, 75, and 90° and the experiment was repeated. The dynamic *in vitro* bioadhesion test was also performed for F8 and A8.

Ex vivo permeation

The permeation of bioadhesive microsponges through gastric mucin was studied using modified vertical Franz diffusion cell as reported in our previous report.[18] The freshly excised abomasum part of goat stomach was procured from a local slaughter house. Gastric mucin was scrapped off carefully by the blunt end of spatula. The mucin sample was purified with repeated changes of distilled water and centrifuged at 2000 rpm for 10 min. The obtained gelatinous mass (500 mg) was reconstituted with 10 ml of phosphate buffer, at a pH of 4.5, and mixed to produce gel. About 1.25 ml of the reconstituted gastric mucin was placed over the dialysis membrane (MW 10–20 kDa) followed by another layer of dialysis membrane placed over it so that mucin was sandwiched between two membranes. The assembly was mounted on the receptor compartment (0.785 cm) of diffusion cell. Receptor compartment was filled with 10 ml of phosphate buffer, at a pH of 4.5. Bioadhesive microsponges (BF8) equivalent to 10 mg of drug were placed in donor compartment and hydrated with phosphate buffer, at a pH of 4.5. The assembly was maintained at 37°C and 2 ml sample was withdrawn from the receptor compartment at hourly intervals till 8 h, replaced with equal volume of phosphate buffer and assayed spectrophotometrically at 251 nm. The procedure was repeated for A8 formulation. The correlation between *in vitro* drug release and *ex vivo* permeation of drug was determined graphically by calculating linear correlation coefficient.

Scanning electron microscopy

Shape and surface morphology of F8, BF8, and A8 was studied by scanning electron microscopy (SEM) (LEO Electron Microscopy, Ltd., Switzerland). The samples were adhered to double adhesive tape stuck to an aluminum stub. These were then coated with gold under argon atmosphere using gold sputter. The microsponges were visualized under various magnifications and images captured.

Differential scanning calorimetry

Thermal analysis of drug, EC, physical mixture thereof, F8, BF8, and A8, was performed by differential scanning calorimetry (DSC) to estimate the interaction, if any between drug and polymer and the state of drug inside the polymer matrix in microsponges. The samples were sealed in aluminum pans and heated at a constant rate of 10°C/min in the range of 0–450°C. Nitrogen purge (60 ml/min) was maintained throughout heating. An intracooler was fitted to assess the thermal behavior of samples.

RESULTS AND DISCUSSION

Preliminary study

Critical micelle concentration

The study was conducted to select the concentration of PVA for preparing microsponges. Initially, the surface tension was 70 dynes/cm at 0.1% w/v of PVA that decreased to 40 dynes/cm at 1% w/v [Figure 1a]. Thereafter, an increase in the surface tension was observed. An increase in the concentration of polymeric surfactant increased the adsorption of available polymer molecules at air–aqueous solution interface that resulted in a

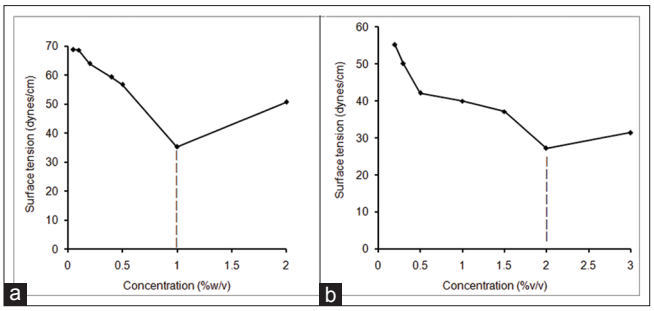

Figure 1: Critical micelle concentration determination plots of (a) polyvinyl alcohol, (b) acconon MC 8-2 EP/NF

decreased surface tension.[19] Correspondingly, CMC was deduced as 1% w/v and presumed to be the concentration that can affect the maximum drug solubilization and hence, it was selected for the experimental design. Furthermore, PVA concentration, above and below the CMC (0.5 and 1.5% w/v, respectively), was selected as lower and higher values for the preparation of microsponges.

In vitro drug adsorption

In vitro drug adsorption study was performed to estimate the optimum time required for stirring to form microsponges with maximum drug entrapment. The percent drug adsorption increased continuously with time. The increment in adsorption was initially rapid, 57.80% in 6 h that slowed down to 63.20% in 8 h. The difference in adsorption was insignificant ($P > 0.01$) at 6 and 8 h mainly because adsorption is a site-specific phenomenon.[20] Limited adsorption sites on the polymer got occupied at 6 h with no significant increase thereafter. Thus, a stirring time of 6 h was selected for formulating microsponges. *In vitro* adsorption study with EC revealed a significant ($P < 0.01$) increase in adsorption on increasing the concentration of EC from 0.3% to 0.9%. On this basis, three concentrations were assumed to be best suited for formulating microsponges.

Preparation of drug-loaded microsponges

Quasi emulsion solvent diffusion method is an established method for the preparation of microsponges with advantages of being easy, reproducible, rapid, and avoids solvent toxicity. Formation of microsponges by this method can be explained in three steps: quassi-emulsion droplets formation, organic solvent diffusion, and droplets solidification.[21] Ethanol served as a good solvent whereas dichloromethane bridged cinnarizine and EC inside the droplets. PVA reduces surface tension, facilitating droplets formulation.[22] With the diffusion of ethanol into the aqueous solution and counter diffusion of PVA, cinnarizine and EC co-precipitated into the droplets. Further, counter diffusion and evaporation decrease the ratio between the good solvent and bridging solvent, accompanying drug solidification on the EC droplets.[23]

Evaluation of microsponges

Product yield

The product yield varied from 70 to 83.17% [Table 2] and was least for F1, made with lower levels of EC and PVA. For a given level of PVA, the product yield increased with an increase in the level of EC. As explained in earlier publications, higher level of EC retarded the diffusion of organic phase thus delaying polymer precipitation. This provided more time for droplets formation and hence higher yields[24] were reported. Less viscous organic phase at lower level of EC resulted in faster removal of solvent causing solidification of drug and polymer before the droplets formation and thereby reducing the yield. For a given level of EC, the product yield was higher at the intermediate level of PVA. At 1% w/v of PVA (CMC), formation of spherical droplets facilitated an increase in the yield. Whereas beyond CMC value, at higher concentration of PVA, its solubility possibly decreased, resulting in lower yield in case of F3, F6, and F9. Thus, F8 made with lowest level of EC and intermediate level of PVA exhibited the maximum percent product yield.

Particle size

The microsponges ranged from 22 ± 2.94 to 70 ± 1.6 μm [Table 2], and the particle size was dependent on the levels of both EC and PVA. The largest particle size of 70 ± 1.6 μm was obtained at a higher level of EC and PVA for F9 formulation. For a given level of PVA, on increasing the level of EC, an increase in the particle size was observed. The increase in particle size is related to increased viscosity at higher level of EC, which resulted in the formation of larger-sized droplets leading to larger microsponges due to an increased surface tension.[25] For a given level of EC, an increase in the level of PVA from −1 to +1 resulted in larger-sized microsponges. The possible explanation was restrained ability of the droplet to divide into smaller particles resulting in the formation of larger microsponges at a higher level of PVA.[26]

Entrapment efficiency

In context to the experimental design, the entrapment efficiency of microsponges on varying EC can be correlated to *in vitro* adsorption study results. An increase in the entrapment efficiency was observed with an increase in the concentration of EC, which indicated adsorption of cinnarizine on the adsorption sites on polymeric fragments used for the fabrication of microsponges. In addition to surface adsorption, the entrapment of drug within the matrix of microsponges led to drug entrapment in the range of 59.9 ± 3.4–82.6 ± 2.3% [Table 2]. The entrapment efficiency was also dependent on PVA concentration. For a given level of EC, low level of PVA (0.5% w/v) resulted in less entrapment of drug that increased at 1% w/v of PVA (corresponding to CMC). Beyond this concentration, further enhancement in entrapment was facilitated by micellar solubilization of drug resulting in highest entrapment at 1.5% w/v of PVA.

In vitro buoyancy

Microsponges have interconnected pores on their surface which provide them buoyancy. Recently, the buoyant behavior of microsponges was proved by Arya and Pathak.[13] On the same lines, formulation F1 to F9 remained buoyant in the test media for 8 h. The low density (0.4 g/cc) of EC[27] coupled with the porous structure of microsponges supported the floating character. The microsponges thus displayed an acceptable

Table 2: Pharmaceutical characteristics of cinnarizine-loaded microsponges

Formulation code	Product yield (%)	Particle size (μm)	Percentage of EE[a]	Buoyancy$_{8h}$ (%)	Percentage of CDR[b]$_{8h}$	Desirability factor	Diffusion exponent (*n*)
F1	70.00	22±2.94	59.9±3.4	62.5±2.8	57.9±1.4	0.473	0.517
F2	80.27	25±1.90	69.6±1.3	70.5±2.4	72.5±1.9	0.542	0.463
F3	72.22	38±1.72	74.6±2.2	80.0±2.9	69.1±1.7	0.594	0.562
F4	75.20	28±1.80	73.4±2.8	72.2±1.6	70.0±2.3	0.544	0.832
F5	82.51	31±1.90	75.7±3.2	77.7±3.1	85.3±1.9	0.622	0.587
F6	77.06	49±1.80	80.3±3.8	83.3±3.5	80.8±1.6	0.675	0.827
F7	79.75	29±1.90	76.8±4.1	76.4±1.7	72.0±1.9	0.651	0.851
F8	82.93	37±1.85	82.4±3.4	82.3±2.5	88.7±2.9	0.725	0.485
F9	81.17	70±1.60	82.6±2.3	80.1±2.3	81.0±2.5	0.700	0.777

[a]EE: Entrapment efficiency, [b]CDR: Cumulative drug release

buoyancy of 62.50% ± 2.8% for F1 to maximum of 83.3% ± 3.5% for F6 followed by F8 [Table 2]. As reported by Sato *et al*.[28] the buoyancy of particle depends on its density and size. With increase in particle size, density decreases that, in turn, exhibits an inverse relation to buoyancy. Hence, the buoyancy of microsponges increased with an increase in particle size, which can be correlated to an increase in the level of EC and PVA and converse was true for smaller-sized microsponges, except for F9 formulation (80.1 ± 2.3), which was made with highest level of EC and PVA. The best possible explanation is attainment of equilibrium state beyond which any further increase in the independent variables did not affect the response.

In vitro drug release

The *in vitro* drug release from microsponges was performed at intermediate fed state pH, 4.5. The promising formulation F8 formulated with high level of EC and intermediate level of PVA exhibited highest drug release of 88.79% ± 2.9% in 8 h in comparison to rest of the formulations [Figure 2], followed by F5 (85.3% ±1.9%; [Table 2]). The drug release from microsponges is predominantly influenced by porosity of microsponges, which is a characteristic feature of the delivery system. The porosity can affect the apparent diffusion coefficient of drug[29] which can ultimately affect drug release. Formation of larger droplets indirectly indicates more interconnected pores that facilitate rapid penetration of dissolution medium into microsponges and helping in dissolution and diffusion of drug from the polymeric matrix.[30] Thus, at higher level of EC viscous phase, coarsening time gets prolonged and larger pores are formed that support the drug release from microsponges. Furthermore, to achieve complete release of drug, incorporation of buffering agents into the microsponges can be considered as a viable option.[31]

To study the mechanism of drug release from microsponges, release data were subjected to various model fittings. The mechanism of drug release was best described by Higuchi's diffusion kinetics with R^2 ranging from 0.9512 to 0.9956. The value of diffusion exponent (*n*) was between 0.463 and 0.851, which is indicative of non-Fickian diffusion model for drug release from microsponges. The mechanisms can be correlated to already established drug release mechanism from microsponges.[32] Polymeric matrix systems are known to be best described by Higuchi model. The result describes diffusion

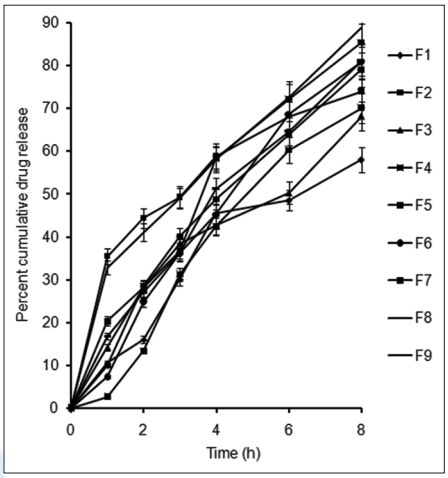

Figure 2: *In vitro* release profiles of cinnarizine from microsponges F1–F9 in phosphate buffer, at a pH of 4.5

and swelling as the mechanisms governing drug release from microsponges as suggested by Mady[33] and Enayatifard *et al*.[34]

Statistical analysis

Considerable amount of useful information reaffirming the utility of statistical design of experiments was generated by employing Design expert software version 9 (Stat-Ease Inc., Minneapolis, USA). Second-order polynomial equations were generated for percent entrapment efficiency, percent buoyancy, and percent correlation of drug release (CDR) by application of one way ANOVA. The insignificant ($P > 0.05$) terms were omitted and the significant polynomial equations are:

$$\%\ \text{Entrapment efficiency} = 75.7 + 6.4X_1 + 2.85X_2 - 1.93X_1X_2 + 1.97X_1^2X_2 - 4.58X_1^2X_2^2 \quad (2)$$

$$\%\ \text{Buoyancy} = 76.14 + 4.30X_1 + 5.39X_2 - 3.43X_1X_2 \quad (3)$$

$$\%\ \text{CDR}_{8h} = 85.30 + 7.42X_1 + 5.39X_2 - 2.03X_1X_2 - 3.91X_1^2 - 9.86X_2^2 - 2.35X_1^2X_2^2 + 1.07X_1X_2^2 \quad (4)$$

Considering these polynomial equations, the responses can be predicted at any value of EC and PVA. Three-dimensional response surface plots were generated to depict the influence

of independent variables simultaneously on dependent variables [Figure 3]. The percent entrapment efficiency increased on simultaneous increase of EC and PVA from lower level to higher level [Figure 3a]. Similarly, percent buoyancy also increased on simultaneously increasing the level of independent variables showing exception for F9 formulation where the buoyancy decreased probably due to attainment of equilibrium in buoyancy [Figure 3b]. Taking into account, the effect of simultaneously varying the levels of EC and PVA, the percent CDR_{8h} was maximum for highest level of EC and intermediate level of PVA [Figure 3c].

Selection of optimized formulation

On the basis of data obtained from response parameters, F8 showed the maximum desirability of 0.725 [Table 2 and Figure 3d] and selected as optimized formulation. The formulation exhibited drug entrapment efficiency of 82% ± 3.4%, buoyancy of 82.3% ± 2.5%, and maximum CDR of 88.79% ± 2.9% after 8 h. Other encouraging pharmaceutical features were smaller particle size (95.5 μm) and zero residual solvent when assayed by gas chromatography-mass spectrophotometry (Agilent 7890 AGC system) 5975C VL MSD, equipped with triple axis detector. The optimized formulation F8 was subjected to bioadhesive coating.

Validation of experimental design

The experimental design was validated by preparing an extra design checkpoint formulation F10. The polynomial equations generated were utilized for calculating the predicted values of the three dependent variables. The close resemblance between predicted and experimental value ascertained the validity of the experimental design. Low values of percentage error [Table 3] between predicted and experimental values affirmed the prognostic ability of the design.

Bioadhesive microsponges

Bioadhesive coating

The bioadhesive coating of optimized formulation was served by capmul GMO-50. Capmul GMO-50 is a mixture of monoglycerides, mainly glyceryl monooleate with some ratios of diglycerides and triglycerides. It is soluble in commonly

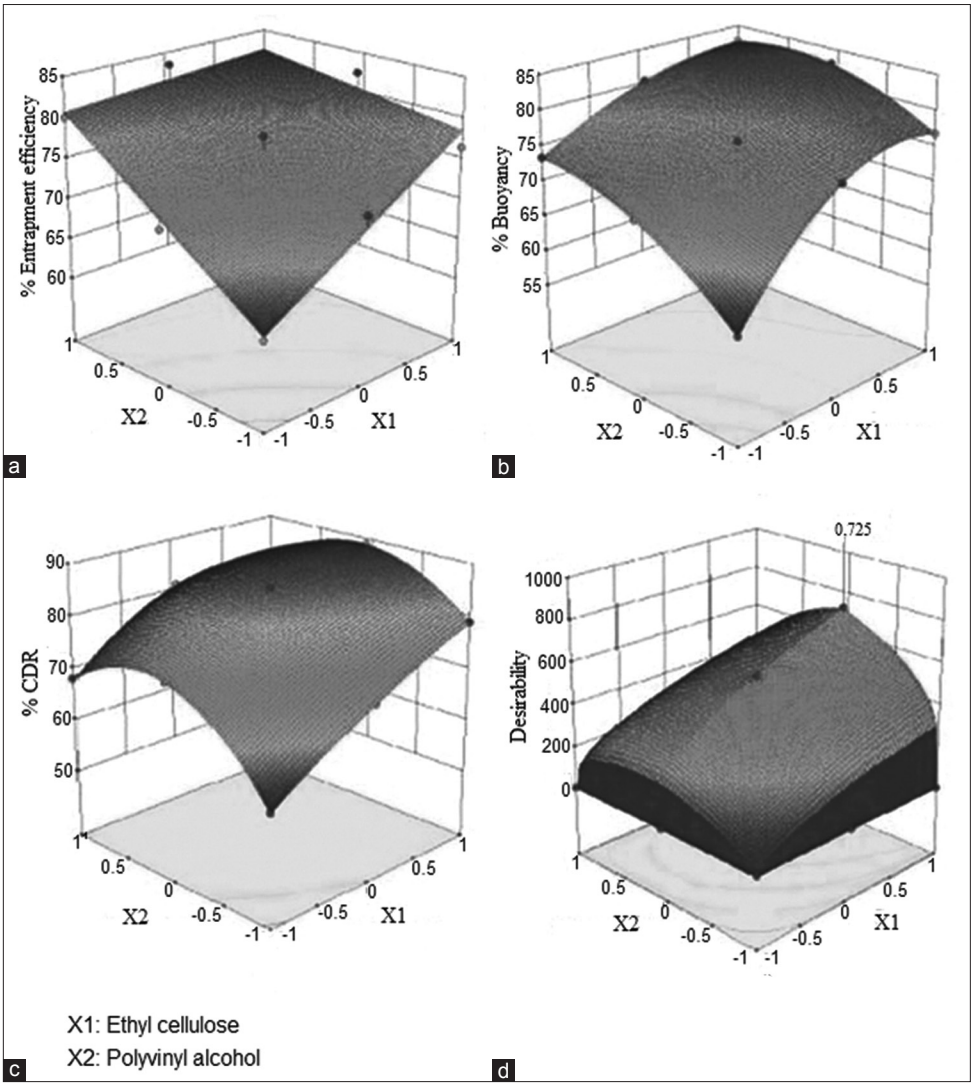

Figure 3: Three-dimensional surface plots for the analysis of response parameters. (a). % Entrapment efficiency, (b). % Buoyancy, (c). % Cummulative Drug Release and (d). Desirability

used organic solvents and meant for coating of various oral formulations.[27] Capmul GMO-50 is known to form liquid crystalline phase in the presence of aqueous media and has mucoadhesive property.[14,35] When exposed to gastric fluid, capmul GMO absorbs water and forms lamellar liquid crystal form followed by cubic phase formation *in situ*. The viscous cubic phase imparts mucoadhesion property.[36] The mechanism for bioadhesion can be described as dehydration and intermixing of mucus joint.[37,38] In addition, the lipids that form liquid crystals in the presence of excess water are known to sustain the release of poorly water-soluble drug.[39] These properties make capmul GMO-50 suitable for bioadhesive coating of microsponges and F8 was thus coated to get BF8.

Bioadhesive raw material

Chemically, acconon MC 8-2 EP/NF is known as PEG-8 caprylic/capric glycerides. It is a mixture of monoesters, diesters, triesters of glycerol and monoesters, and diesters of polyoxyethylene glycol. The composition contains free macrogols as well. Caprylic acid is chemically eight carbons, saturated fatty acid, which may be claimed as bioadhesive in nature.[40] Apart from this, polyethylene glycol/macrogol had already been assessed to impart bioadhesive character. In addition, the presence of PEG polymer on the mono or diesters of glycerides imparts suitable water solubility to glycerides,[41] which serves to be advantageous upon contact to mucus. Based on these reports, acconon MC8-2 EP/NF was utilized as a novel bioadhesive raw material for microsponges development. Its CMC was experimentally deduced at 2% v/v [Figure 1b] and was used for formulating microsponges. The process variables of optimized formulation (F8), with slight modification, were used for the fabrication of microsponges using acconon MC 8-2. The amount of EC was reduced to 600 mg instead of 900 mg, because at latter concentration, irregularly-shaped droplets were formed. This may be due to low surfactant activity of acconon: CMC of 2% w/v and HLB value of 14.[42] Thus, the extent of reduction in the interfacial tension was less and consequently high viscosity organic phase restricted the formation of spherical droplets. Another process variable modulated was the temperature. At the temperature used for preparing F8, the microsponges adhered to the walls of beaker and magnetic bead, thus decreasing the yield as well as did not allow splitting of droplets leading to large microparticles. Thus, for fabrication of A8 (acconon MC 8-2 based microsponges), 600 mg of EC was employed at a temperature of 20 ± 2°C.

Evaluation of bioadhesive microsponges

Entrapment efficiency and in vitro buoyancy

The entrapment efficiency of bioadhesive microsponges was 79.2 ± 2.6 and 78.5 ± 1.1% for BF8 and A8, respectively [Table 4], that is less than F8. The total dry mass of microsponges increased due to deposition of bioadhesive coating material over its surface in case of BF8, resulted in decreased percent entrapment efficiency. Insignificantly lower ($P > 0.05$) entrapment in case of A8 can be attributed to fewer adsorption sites available to entrap drug at lower amount of EC. *In vitro* buoyancy of BF8 and A8 was 81.6 ± 3.7% and 84.6 ± 1.9%, respectively [Table 4]. Insignificant difference confirmed the viability of bioadhesive microsponges to remain buoyant under specific conditions. The results also assessed the ability of microsponges prepared with acconon to serve the purpose of floating similar to F8/BF8.

Table 3: Comparison of predicted and experimental data of extra design checkpoint formulation

Code	Response	Predicted value	Experimental value	Percentage error
F10 (extra design check point)	% EE	79.83	78.62	1.51
	% Bouyancy$_{8h}$	80.14	81.29	1.43
	%CDR$_{8h}$	84.92	82.97	2.29

CDR: Cumulative drug release, EE: Entrapment efficiency

Table 4: Evaluation parameters of bioadhesive microsponges in reference to optimized uncoated microsponges

Formulation code	Particle size (μm)	Entrapment efficiency (%)	Buoyancy$_{8h}$ (%)	% CDR$_{8h}$
F8 (optimized uncoated)	95.9±65.6	82.8±3.4	82.3±2.5	88.7±2.9
BF8 (bioadhesive coated)	126.5±55.6	79.2±2.6	81.6±3.7	87.2±3.5
A8 (bioadhesive)	201.9±59.6	78.5±1.1	84.6±1.9	82.9±3.2

CDR: Cumulative drug release

In vitro drug release

The *in vitro* drug release from BF8 was 87.2 ± 3.5% which is comparable to 88.79 ± 2.9% in 8 h, which clearly pronounces nonhindrance of coating layer on drug release [Table 4] and it is supported by the similarity factor (*f2*) of 86.15 between the profiles of F8 and BF8. Capmul GMO is documented to form cubic phase in the presence of aqueous media[35] that has affinity for hydrophilic as well as lipophilic drugs, causing release of drug from pores by diffusion mechanism. On the other hand, percent CDR at 8 h from A8 (82.9% ±3.2%) was lower than BF8 [Figure 4] with a similarity factor (*f2*) of 61.04 and dissimilarity factor (*f1*) of 9.24, proving the effectiveness of acconon MC 8-2 as a raw material for microsponges preparation.

Floating systems are known to be active when administered in fed-state conditions. Depending on the type of meal, the pH of fed state can vary from 2.5 to 6.5 correspondingly to low, intermediate, and high fed state pH, respectively.[43] When the drug release from optimized microsponges (F8) was examined at different fed state pH, the decrease in the release of cinnarizine was observed on shifting the pH from 2.5 to 6.5 [Figure 5a]. The difference was insignificant for pH 2.5 and 4.5 ($P > 0.05$), whereas drug released at pH 4.5 and 6.5 was dissimilar, $f1 = 19.81$. A decrease in drug release was observed from 88.79% to 79.81% for F8. Similarly, the microsponges prepared with acconon MC 8-2 were also assessed for the effect of pH on drug release. The release was highest (84.35%) at pH 2.5, corresponding to high gastric acidity. On increasing the pH to 4.5, no significant difference ($P > 0.01$)

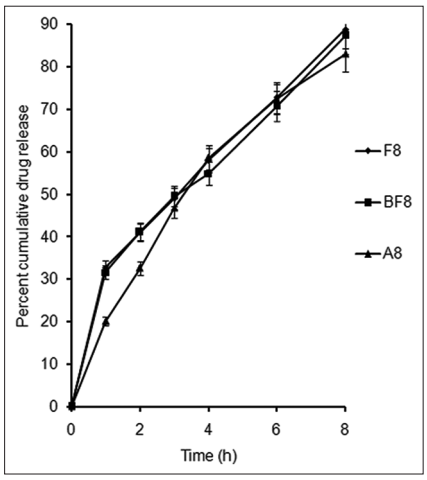

Figure 4: Comparative *in vitro* drug release profiles of F8, BF8, and A8 in phosphate buffer, at a pH of 4.5

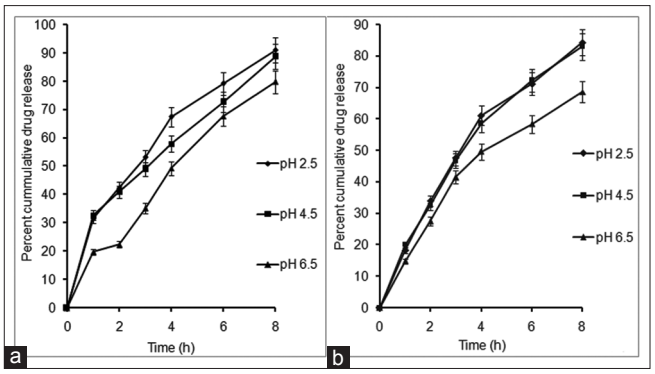

Figure 5: Effect of pH on release of cinnarizine from (a) optimized formulation, F8 and (b) A8 formulation

was observed. Whereas further increasing the pH showed a significant decrease in release ($P < 0.01$), giving a maximum release of 82.9% ± 3.2% in 8 h [Figure 5b]. This difference was proved by dissimilarity factor of 16.89. The difference is attributable to the basic nature of cinnarizine, pKa = 8.4.[44] At lower pH, cinnarizine is partitioned in the dissolution media giving higher drug release. This pH-dependent dissolution pattern of cinnarizine is of great interest to researchers as it affects the absorption of the drug.

Dynamic in vitro bioadhesion

The study was performed to assess the bioadhesivity of BF8 and A8 in reference to F8. The features of designed equipment have been explained in our previous publication.[18] Broadly speaking, the equipment simulates the conditions of stomach more appropriately than those of the static angle assembly, and the results can be expected to be close to the physiological conditions. At the start of the test, none of the microsponges (BF8) showed movement when plate A was made to move at 30, 45, 60, and 75° angles. At 90°, only one microsponge rolled to a distance of 0.7 cm in case of BF8 in comparison to two microsponges that rolled down >8.5 cm for F8. This manifested increased bioadhesivity for BF8. In contact with mucus, the GMO coating got hydrated, forming cubic-phase liquid crystals[37] that can be correlated to the formation of stiff gel *in situ*. This provided an effective adherence to the mucus.

Considering A8 formulation, not a single microsponge slided even at extreme 90° angle. This indicated a novel concept of strong bioadhesivity accountable to acconon used for microsponges fabrication. The contribution of acconon to improve the bioadhesivity of A8 may be attributed to the presence of free macrogols in its composition. The macrogols are adhesive in nature and have been reported as bioadhesive polymer.[45,46] Improved bioadhesivity can also be attributed to the low amount of EC used in A8 that offered less hindrance to bioadhesion.[47] Concluding, A8 made with acconon unveiled good bioadhesion property and the method eliminates additional coating step for conferring bioadhesivity, thus minimizing the loop points associated with coating step.

Ex vivo permeation

The ability of cinnarizine to permeate through gastric mucin may account for its absorption in gastric cavity that can be achieved by increased contact time. Thus, the bioadhesive microsponges were assessed for permeation ability. The cumulative drug permeation (CDP) from bioadhesive-coated microsponges (BF8) through gastric mucin was found to be 63.16% in 8 h that followed zero-order kinetics ($R^2 = 0.9847$) and indicative of high drug absorption. On the other hand, A8 exhibited less permeation of 56.74% in 8 h and followed zero-order kinetics with R^2 value of 0.9938 9 [Figure 6a]. Although the CDP was decreased in case of A8 than that of BF8, the profiles from the two bioadhesive formulations (A8 and BF8) can be stated similar with a similarity factor (*f2*) of 58.16. On establishment of (CDR) with the correlation of drug permeated (CDP), a correlation coefficient of 0.9718 (slope = 0.9510) was observed for BF8 [Figure 6b]. The value of slope approximating one suggested that almost the entire amount of drug released from BF8 is capable of permeating across the gastric mucin, *in vivo*, whereas a slope of 0.7824 observed for A8 with a correlation coefficient of 0.9701 (CDP vs. CDR; [Figure 6c]) suggests that more amount of drug would be released than would get permeated. Relatively lower permeation from A8 can be improved by the incorporation of permeation enhancer in the microsponges. Hydrophilic thiolated polymeric permeation enhancers that are generally not absorbed are nontoxic and are known to improve permeation by increasing the mucus residence time of permeation enhancers.[48] The results affirm the utility of acconon MC 8-2 EP/NF for preparing bioadhesive microsponges.

Dynamic laser scattering

The mean particle size of F8 was found to be 95.6 μm, which was increased to 126.5 μm in case of BF8 [Table. 5]. This manifested the deposition of coating material over the surface of microsponges, thus increasing their size. The particle size distribution was bimodal [Figure 7a] with specific surface area of 2980 cm^2/ml for F8 that was transformed to unimodal distribution [Figure 7b] on coating with GMO, and the specific

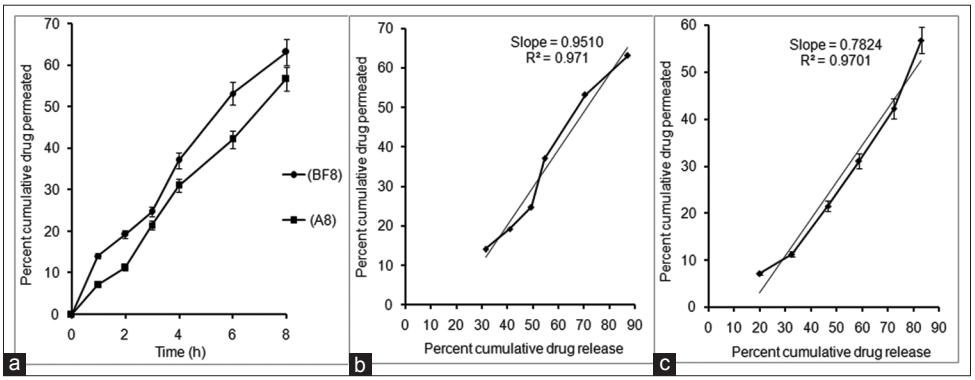

Figure 6: *Ex vivo* permeation profiles of BF8 and A8 across gastric mucin (a) correlation profile between cumulative drug release and cumulative drug permeated from BF8 (b) and A8 (c)

Table 5: Particle size data for optimized uncoated (F8), bioadhesive-coated (BF8), and bioadhesive (A8) obtained by dynamic laser scattering

Parameter	F8	BF8	A8
Mean (μm)	95.9	126.5	201.9
Median (μm)	84.4	144.1	189.6
Mode (μm)	168.9	168.9	203.5
Specific surface area (cm^2/ml)	2980	2528	314.5
SD (μm)	65.6	55.6	59.6
Variance (μm)	4314	3096	3559
IQCS	0.20	−0.35	−0.02
d_{10} (μm)	15.5	31.8	153.9
d_{90} (μm)	183.5	184.7	229.9
Skewness (μm)	0.13	−0.84	2.38
	Right skewed	Left skewed	Right skewed
Kurtosis (μm)	−1.51	−0.41	5.12
	Platykurtic	Platykurtic	Leptokurtic
Span (μm)	2.01	1.05	0.40

IQCS: Interquartile coefficient of skewness, SD: Standard deviation

surface area was reduced to 2528 cm^2/ml. The results were supported by lower value of standard deviation in case of BF8 which reflects uniformity in size distribution. This can further be justified by the lower value of span (1.05) for BF8 formulation, confirming narrow particle size distribution[49] in comparison to F8 (span = 2.01). This indicates a decrease in polydispersity of coated microsponges, tending toward normal particle size distribution. Skewness and kurtosis are significant parameters to measure the degree of departure from normal frequency. The data indicate a shift from right skewed for F8 to left skewed distribution for BF8. Both the F8 and BF8 formulations were platykurtic with a relatively more peaked distribution for BF8 formulation.

The particle size distribution of A8 was more uniform [Figure 7c] in comparison to F8 and BF8, with a mean particle size of 201.9 μm. Larger particle size may be attributed to the presence of free macrogols due to which the formed droplets were not able to dissociate easily into smaller particles. Other significant micromeritic characteristics are narrow size distribution with specific surface area of 314.5 cm^2/ml (span = 0.400 μm and kurtosis = 5.122) and positive skewness of 2.389. The peak distribution was leptokurtic, tending toward normal distribution as indicated by an IQCS value of −0.02. Thus, microsponges formed with acconon displayed less variability in particle size distribution than BF8 and F8. All the parameters quantified manifested the supremacy of A8 formulation over others in terms of micromeritics.

Scanning electron microscopy

The scanning electron micrographs of F8 indicated spherical-shaped microsponges [Figure 8a]. Image of a fractured microsponge revealed porous polymeric matrix of the microsponges, affirming its internal structure. At higher resolution, the micrograph of outer surface revealed numerous tiny pores over it [Figure 8b]. The micrograph of BF8 revealed spherical-shaped smooth-surfaced microsponges [Figure 8c], and the surface morphology indicated deposition of coating material over the surface of microsponges [Figure 8d]. The images showed appearance of crystals of cinnarizine on the surface of microsponges, which was further indicated by DSC results (discussed later). The SEM images of A8 revealed formation of spheroidal microsponges with lack of spherical shape [Figure 8e]. The magnified view suggested rugged surface with minute pores [Figure 8f]. The shape may be further improved by the optimization of formulation/fabrication variables and it is under consideration in our research efforts.

DIFFERENTIAL SCANNING CALORIMETRY

The DSC thermograms were interpreted to identify interaction if any present between drug and excipients and the physical state of drug in microsponges. The thermogram of pure cinnarizine revealed a sharp exothermic peak at 123.8°C, representing the melting point in crystalline state [Figure 9a]. The thermogram for EC showed a blunt and small exothermic peak at 182.3°C with enthalpy of 2.85 J/g [Figure 9b] corresponding to the amorphous nature of EC. In the thermogram of the physical mixture [Figure 9c], the peaks corresponding to cinnarizine and EC were retained suggesting compatibility between the two. The thermogram of optimized formulation (F8) showed

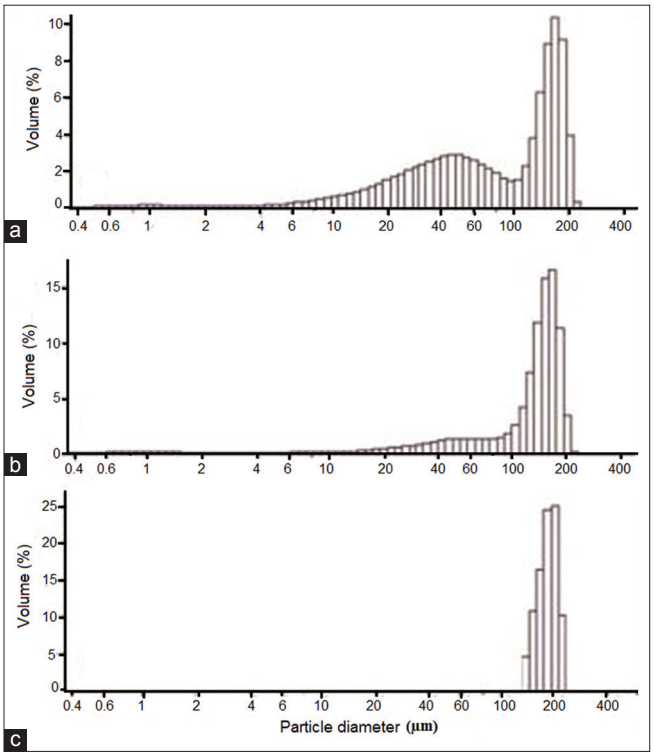

Figure 7: Particle size distribution of (a) optimized formulation, F8 (b) BF8, and (c) A8

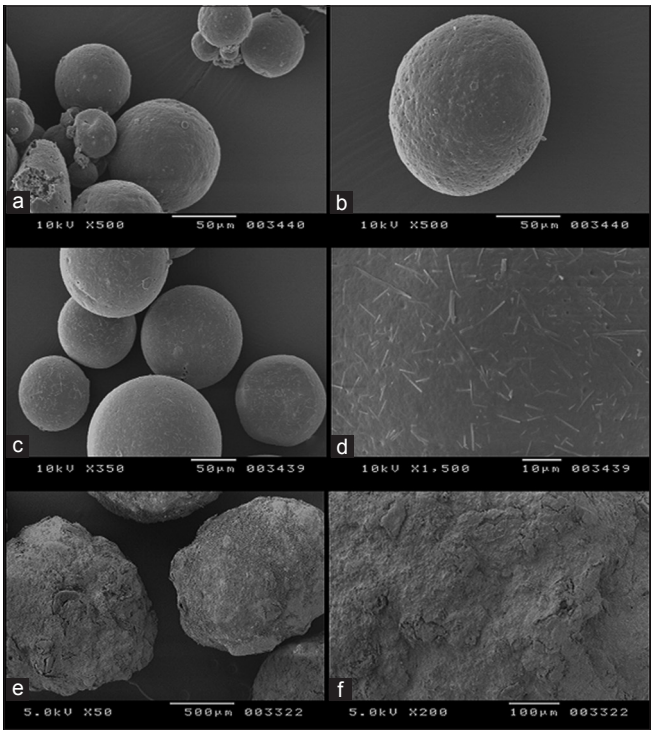

Figure 8: Scanning electron micrographs (a) intact microsponges, (b) surface view of microsponges, (c) bioadhesive-coated microsponges, (d) surface view of bioadhesive-coated microsponges, (e) microsponges of A8 formulation, (f) surface view of A8 microsponges

peaks at 107.4 and 160.9°C that correspond to cinnarizine and EC, respectively [Figure 9d]. This suggested the presence of crystals of cinnarizine. The pronounced shifting of the peak of the cinnarizine and EC was predictive of some kind of interaction. The short broad peak of cinnarizine with shift in melting point is suggestive of partial molecular dispersion of drug in addition to drug crystals in the microsponge's matrix, and also indicates some interaction between drug and polymer depending on the drug entrapment mechanism. The higher value of diffusion coefficient (*n*) for *in vitro* release data [Table 2] was also in agreement with some kind of interaction. The interaction between drug and polymer may increase the polarity in the microsponges' structure, which leads to increase the value of diffusion exponent (*n*) as explained by Mady and Mabrouk.[50] The thermogram of capmul GMO (bioadhesive coating material) displayed a broad melting range of 227.7–291.0°C that peaked at 263.3°C [Figure 9e] indicating its melting point. The thermogram of bioadhesive-coated microsponges [Figure 9f] showed a peak at 100.5°C, which may be for drug. The broadening of peak along with further shifting with respect to that in optimized formulation (F8) can be attributed to the effect of coating material. On increasing the temperature, another rise at about 200°C was assumed to be of capmul GMO. This suggested for deposition of capmul GMO over the surface of microsponges.

The thermogram of microsponges A8 [Figure 9g] prepared using acconon MC 8-2 EP/NF displayed appearance of peaks at 122.4°C and 176.2°C corresponding to drug and polymer, respectively, when compared to reference peaks. The appearance of small peak at 122°C suggested for the presence of traces of crystalline cinnarizine in the microsponges. The difference in the thermogram of F8 and A8 is suggestive of impact of surfactant used in the respective formulations. PVA used as a surfactant in F8 is presumed to affect crystallinity of the drug resulting into small needle-like appearance (as shown in SEM results), thus shifting the melting point of cinnarizine. Such kind of effect of surfactant has been explained by Khalid *et al*.,[51] wherein the spherical particles changed into needle-like appearance in the presence of surfactant. An experiment conducted to crystallize cinnarizine in the presence of PVA verified the above-mentioned presumption (photomicrographs not shown). Correspondingly, fine needle-shaped crystal deposits were observed on the surface of F8.

CONCLUSION

The study clearly demonstrated the successful development of bioadhesive floating microsponges. The involvement of CMC to optimize the concentration of polymeric surfactants suggested a logical approach to select the surfactant concentration for the fabrication of microsponges. The bioadhesive coating employing capmul GMO provided an effective adherence to gastric mucus layer without hindering the release of cinnarizine from microsponges. Assessment of acconon MC 8-2 EP/NF as polymeric surfactant for the preparation of microsponges emerged as a novel approach. These microsponges showed a good bioadhesive property without the need of bioadhesive coating and eliminated the loop points associated with coating step. Thus,

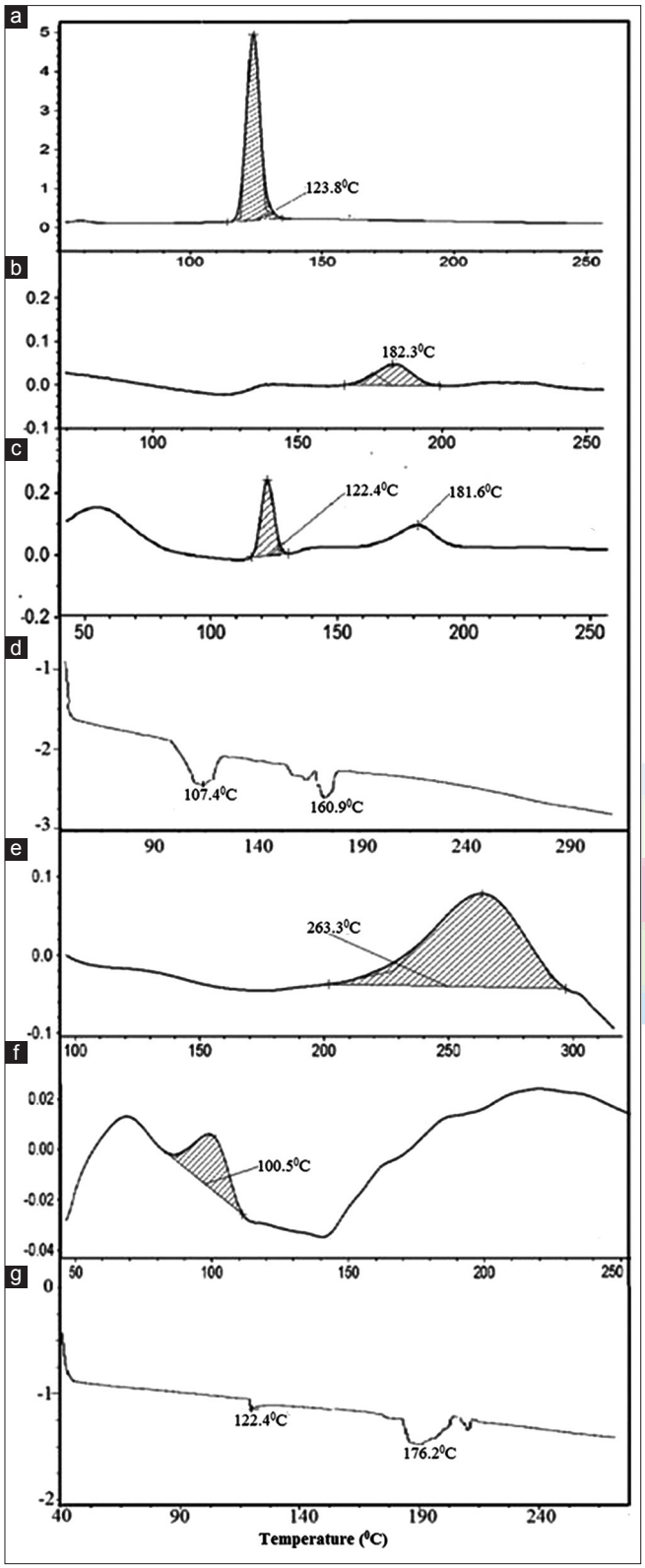

Figure 9: Differential scanning calorimetry thermograms (a) cinnarizine, (b) ethyl cellulose, (c) physical mixture, (d) optimized formulation, (e) Capmul GMO, (f) bioadhesive-coated microsponges (BF8), (g) A8 formulation

set forth a novel approach for preparing low-density bioadhesive microsponges. Acconon is also known to enhance bioavailability and efforts are being dedicated to assess the improvement in bioavailability *in vivo*.

Financial support and sponsorship

Nil.

Conflicts of interest

None declared.

REFERENCES

1. Shahba AA, Mohsin K, Alanazi FK. Novel self-nanoemulsifying drug delivery systems (SNEDDS) for oral delivery of cinnarizine: Design, optimization, and *in-vitro* assessment. AAPS PharmSciTech 2012;13:967-77.
2. Ogata H, Aoyagi N, Kaniwa N, Ejima A, Sekine N, Kitamura M, *et al*. Gastric acidity dependent bioavailability of cinnarizine from two commercial capsules in healthy volunteers. Int J Pharm 1986;29:113-20.
3. Ogata H, Aoyagi N, Kaniwa N, Ejima A, Kitaura T, Ohki T, *et al*. Evaluation of beagle dos as animal model for bioavailability testing of cinnarizine capsules. Int J Pharm 1986;29:121-6.
4. Burton PS, Goodwin JT, Vidmar TJ, Amore BM. Predicting drug absorption: How nature made it a difficult problem. J Pharmacol Exp Ther 2002;303:889-95.
5. Solanki B, Patel R, Barot B, Parijiya P, Shelat P. Multiple unit dosage form: A review. Ph Tech Med 2012;1:11-21.
6. Goyel M, Prajapati R, Purohit KK, Mehta SC. Floating drug delivery system. J Curr Pharm Res 2010;5:7-18.
7. Varshosaz J, Tabbakhian M, Zahrooni M. Development and characterization of floating microballoons for oral delivery of cinnarizine by a factorial design. J Microencapsul 2007;24:253-62.
8. Patnaik A, Mantry S. Formulation and evaluation of gastroretentive floating microsphere of cinnarizine. Asian J Pharm Clin Res 2012;5:100-9.
9. Patel JK, Patil PS, Sutariy AV. Formulation and characterization of mucoadhesive microparticles of cinnarizine hydrochloride using supercritical fluid technique. Curr Drug Deliv 2013;10:317-25.
10. Charde MS, Ghanawat PB, Welankiwar AS, Kumar J, Chakole RD. Microsponge: A novel new drug delivery system: A review. Int J Adv Pharm 2013;2:63-70.
11. Nokhodchi A, Jelvehgari M, Siahi MR, Mozafari MR. Factors affecting the morphology of benzoyl peroxide microsponges. Micron 2007;38:834-40.
12. Kaity S, Maiti S, Ghosh AK, Pal D, Ghosh A, Banerjee S. Microsponges: A novel strategy for drug delivery system. J Adv Pharm Technol Res 2010;1:283-90.
13. Arya P, Pathak K. Assessing the viability of microsponges as gastro retentive drug delivery system of curcumin: Optimization and pharmacokinetics. Int J Pharm 2014;460:1-12.
14. Upadhyay MS, Pathak K. Glyceryl monooleate-coated bioadhesive hollow microspheres of riboflavin for improved gastroretentivity: Optimization and pharmacokinetics. Drug Deliv Transl Res 2013;3:209-23.
15. Yadav JB. Advanced Practical Physical Chemistry. 16th ed. India: Krishna Prakash Media (P) Ltd.; 1998.
16. Comoglu T, Gönül N, Baykara T. Preparation and *in vitro* evaluation of modified release ketoprofen microsponges. Farmaco 2003;58:101-6.
17. Gohel MC, Mehta PR, Dave RK, Bariya NH. A more relevant dissolution method for evaluation of floating drug delivery

system. Dissolution Technol 2004;11:22-5.

18. Rajput P, Singh D, Pathak K. Bifunctional capsular dosage form: Novel funicular cylindrical gastroretentive system of clarithromycin and immediate release granules of ranitidine HCl for simultaneous delivery. Int J Pharm 2014;461:310-21.
19. Panda S, Mohanty GC, Roy G, Sahoo K. Determination of surface tension, optical rotativity and refractive index of polymer polyvinyl alcohol PVA (Mw=1.25,000), in various solvents at different concentrations. Lat Am J Phys Educ 2011;5:734-40.
20. Srivastava R, Kumar D, Pathak K. Colonic luminal surface retention of meloxicam microsponges delivered by erosion based colon-targeted matrix tablet. Int J Pharm 2012;427:153-62.
21. Orlu M, Cevher E, Araman A. Design and evaluation of colon specific drug delivery system containing flurbiprofen microsponges. Int J Pharm 2006;318:103-17.
22. Maqhsoodi M. Formation of pores in microparticles prepared by quassi emulsion solvent diffusion method. AAPS PharmSciTech 2009;10:120-8.
23. Li WI, Anderson KW, Deluca PP. Kinetic and thermodynamic modeling of the formation of polymeric microspheres using solvent extraction/evaporation method. J Control Release 1995;37:187-98.
24. Lee JH, Park TG, Choi HK. Development of oral drug delivery system using floating microspheres. J Microencapsul 1999;16:715-29.
25. Nokhodchi A, Jelveghari M, Siahi M, Dastmalchi S. The effect of formulation type on the release of benzoyl peroxide from microsponges. Iran J Pharm Sci 2005;1:131-42.
26. Jelvehgari M, Siahi-Shadbad MR, Azarmi S, Martin GP, Nokhodchi A. The microsponge delivery system of benzoyl peroxide: Preparation, characterization and release studies. Int J Pharm 2006;308:124-32.
27. Rowe RC, Sheskey JP, Owen SC. Handbook of Pharmaceutical Excipients. 5th ed. India: Pharmaceutical Press; 2006.
28. Sato Y, Kawashima Y, Takeuchi H, Yamamoto H. Physicochemical properties to determine the buoyancy of hollow microspheres (microballoons) prepared by the emulsion solvent diffusion method. Eur J Pharm Biopharm 2003;55:297-304.
29. Siepmann J, Faisant N, Akiki J, Richard J, Benoit JP. Effect of the size of biodegradable microparticles on drug release: Experiment and theory. J Control Release 2004;96:123-34.
30. Maiti S, Kaity S, Ray S, Sa B. Development and evaluation of xanthan gum-facilitated ethyl cellulose microsponges for controlled percutaneous delivery of diclofenac sodium. Acta Pharm 2011;61:257-70.
31. Mehta DM, Parejiya PB, Barot BS, Shelat PK. Investigation of the drug release modulating effect of acidifiers in modified release oral formulation of cinnarizine. Asian J Pharm Sci 2012;7:193-201.
32. Jain V, Singh R. Dicyclomine – Loaded eudragit based microsponges with potential for colonic delivery: Preparation and characterization. Trop J Pharm Res 2010;9:67-72.
33. Mady O. Studying the effect of dispersed drug crystal in the organic phase on the encapsulation by solvent evaporation technique; (4) dependent models as tools for studying the drug release. World J Pharm Sci 2014;2:549-64.
34. Enayatifard R, Saeedi M, Akbari J, Tabatabaee YH. Effect of hydroxypropyl methylcellulose and ethyl cellulose content on release profile and kinetics of diltiazem hcl from matrices. Trop J Pharm Res 2009;8:425-32.
35. Kumar M K, Shah MH, Ketkar A, Mahadik KR, Paradkar A. Effect of drug solubility and different excipients on floating behaviour and release from glyceryl monooleate matrices. Int J Pharm 2004;272:151-60.
36. Sallam AS, Khalil E, Ibrahim H, Freij I. Formulation of an oral dosage form utilizing the properties of cubic liquid crystalline phases of glyceryl monooleate. Eur J Pharm Biopharm 2002;53:343-52.
37. Nielsen LS, Schubert L, Hansen J. Bioadhesive drug delivery systems. I. Characterisation of mucoadhesive properties of systems based on glyceryl mono-oleate and glyceryl monolinoleate. Eur J Pharm Sci 1998;6:231-9.
38. Liu Z, Lu W, Qian L, Zhang X, Zeng P, Pan J. *In vitro* and *in vivo* studies on mucoadhesive microspheres of amoxicillin. J Control Release 2005;102:135-44.
39. Boyd BJ, Khoo SM, Whittaker DV, Davey G, Porter CJ. A lipid-based liquid crystalline matrix that provides sustained release and enhanced oral bioavailability for a model poorly water soluble drug in rats. Int J Pharm 2007;340:52-60.
40. Hansen J, Neilsen LS, Norling T. Use of fatty acid esters as bioadhesive substances. U.S. Patent 5955502A; 21 September, 1999.
41. Gizurarson S. A bioadhesive agent. E.P. Patent 1480673A1; 1 December, 2004.
42. Anjana D, Nair KA, Somashekara N, Venkata M, Sripathy R, Yelucheri R, *et al*. Development of curcumin based ophthalmic formulation. Am J Infect Dis 2012;8:41-9.
43. Chauhan MS, Kumar A, Pathak K. Osmotically regulated floating asymmetric membrane capsule for controlled site-specific delivery of ranitidine hydrochloride: Optimization by central composite design. AAPS PharmSciTech 2012;13:1492-501.
44. British Pharmacopoeia, Commission on Human Medicine Pursuant. The Stationary Office, London; 2004.
45. Roy S, Pal K, Anis A, Pramanik K, Prabhakar B. Polymers in mucoadhesive drug delivery system: A brief note, designed monomers and polymers. Designed Monomers Polym 2009;12:483-95.
46. Muttukumaran M, Dhachinamurthi D, Chandra Shekhar KB, Sriram N. Polymers in mucoadhesive drug delivery system: A brief note. Int J Pharm Ind Res 2011;1:122-7.
47. Yellanki SK, Singh J, Syed JA, Bigala R, Goranti S, Nerella NK. Design and characterization of amoxicillin trihydrate mucoadhesive microspheres for prolonged gastric retention. Int J Pharm Sci Drug Res 2010;2:112-4.
48. Junginger HE. Polymeric permeation enhancer. Barriers, Strategies and Future Trends. In: Andreas Bernkop-Schnürch, editors. Oral Delivery of Macromolecular Drugs. US: Springer; 2009.
49. Gupta PS, Sharma V, Pathak K. Melt sonocrystallized piroxicam for oral delivery: Particle characterization, solid state analysis, and pharmacokinetics. Expert Opin Drug Deliv 2013;10:17-32.
50. Mady OY, Mabrouk M. Studying the effect of surfactant on eudragit RS 100 microspheres prepared by solvent evaporation technique. Mansura J Pharm Sci 1997;13:30.
51. Khalid M, Mujahid M, Amin S, Rawat RS, Nusair A, Deen GR. Effect of surfactant and heat treatment on morphology, surface area and crystallinity in hydroxyapatite nanocrystals. Ceram Int 2013;39:39-50.